

# Prediction of Unusual Plasma Discharge by Using Support Vector Machine

NAKAGAWA Shota<sup>a</sup>, HOCHIN Teruhisa<sup>a,\*</sup>, NOMIYA Hiroki<sup>a</sup>, NAKANISHI Hideya<sup>b</sup>, SHOJI Mamoru<sup>b</sup>

<sup>a</sup>*Kyoto Institute of Technology, Goshokaido-cho, Matsugasaki, Sakyo-ku, Kyoto 606-8585, Japan*

<sup>b</sup>*National Institute for Fusion Science, 322-6 Oroshi-cho, Toki 509-5292, Japan*

---

## Abstract

This paper proposes a method for predicting an unusual emission of visible light inside the plasma vessel by using a Support Vector Machine (SVM) because the unusual emission of visible light can be caused by unexpected heating on the vessel surface. This emission must be predicted to avoid unexpected situations in which it causes some damage to the vessel. The light reflected from the divertor tiles is used as the unusual emission light. This study aims to predict such unusual emission through pictures before the start of the unusual emission, regardless of the plasma physics. This study experimentally confirms that the unusual emission of visible light inside the plasma vessel can be predicted with an accuracy rate of 96.4%, and approximately 0.3 seconds before the start of an unusual emission.

*Keywords:* plasma, prediction, support vector machine, unusual emission

---

## 1. Introduction

At the National Institute for Fusion Science (NIFS), high-temperature plasma experiments have been conducted using the Large Helical Device (LHD) [1], which is a superconducting plasma confinement device that adopts a heliotron  
5 magnetic configuration. During these experiments, visible light emissions are

---

\*Corresponding author  
Email address: hochin@kit.ac.jp (HOCHIN Teruhisa)

observed after ignition of plasma discharges. Fig. 1 shows an example of visible light emission. At NIFS, images of visible light inside the plasma vessel have been recorded as videos and stored in disk devices [2]. The duration of a plasma video ranges from a few seconds to one hour. More than 100,000 videos are  
10 currently stored.

In LHD experiments, unexpected heat influxes to plasma-facing walls occur occasionally, which might incur severe damages to the vacuum vessel. In such situations, intense light emissions from the red-heat wall tiles are incidental, so that we must identify them in the LHD video data. Accordingly, this study  
15 investigated ways to predict such undesirable situations in advance so as to elicit evasive actions.

Disruption phenomena have been extensively investigated in several tokamak experiments. Some studies have attempted to detect disruption by taking signal processing approaches, including the Wavelet transformation [3–6]. Others have  
20 attempted to predict disruption by using machine learning methods, among which the Support Vector Machine (SVM) and the Neural Network (NN) stand out [7–14].

Nakagawa *et al.* proposed methods for predicting unusual light emission using the SVM and the NN [7, 15–17]. They used the light reflected from divertor  
25 tiles as the unusual visible light. Fig. 2 shows an example of the light, where the gold or yellow curves can be seen in the upper right quadrant. This represents the light emitted by the overheated divertor tiles, which appears to be reflected on the inner surface of the vacuum vessel. The divertor is directly exposed to particle and heat fluxes from the plasma, which are transported along  
30 magnetic field lines. The divertor acts by exhausting impurities and removing the heat load from the plasma. Fig. 3 depicts the sectional view of the LHD including divertors [18]. Divertors are placed apart from the plasma and are placed below the plasma shown in Fig. 2. The objective of this study is the prediction of this unusual emission through pictures before the start of unusual  
35 emission, regardless of plasma physics. Notably, this unusual visible light is

often observed. As sufficient number of frames<sup>1</sup> including this light can be obtained, machine learning methods, which usually require a considerable amount of data for precise estimation, can be used in estimating this light. This study also considers this light as an unusual visible light. In addition, Nakagawa *et al.* used plasma videos rather than plasma parameters because observations of unusual light emissions are never intended to analyzing the plasma behaviors, but to investigate the possibility of using this method for predicting unusual light emission phenomena only by using a time series of camera pictures. They showed that the performance of the method using the SVM is better than that using the NN [15]. The probability of an unusual emission, however, fluctuates too much to be used in the prediction. Although they attested the performance of the method, their evaluation was still preliminary.

This study improves the SVM method proposed by Nakagawa *et al.* [15]. The proposed method calculates the probability of unusual emission by taking the mean values of the probability values of several frames. This study also precisely evaluates the proposed method to show its effectiveness.

The remainder of this paper is organized as follows. Section 2 presents the existing literature. Section 3 describes the study methods. Section 4 evaluates the proposed method. Section 5 discusses the results. Finally, Section 6 concludes the paper.

## 2. Related works

### 2.1. Support vector machine

SVMs comprise the supervised machine learning methods [19], which use training data in the learning process. An SVM attempts to find the hyperplane by dividing data into two sub-spaces with the maximum distance between the data closest to the hyperplane. This hyperplane is called the separate hyperplane. The distance between the hyperplane and the data is called the margin.

---

<sup>1</sup>A frame is one of the still images constituting a video.

The data closest to the hyperplane are called support vectors. This situation is illustrated in Fig. 4. As the data are divided into two subsets of data, there are  
65 two types of support vectors: those for a data subset and a different data subset. These are often called positive and negative support vectors, respectively.

When data cannot be divided linearly into the original space, a mapping function called kernel can be used for mapping the data to a higher-dimensional space, where the data can be divided linearly (Fig. 5). Gaussian kernel and  
70 Polynomial kernel are popular kernels.

## 2.2. Disruption prediction using machine learning

In a tokamak device, disruption is an event in which the plasma suddenly shuts down.

Many disruption prediction methods using machine learning methods have  
75 been reported. Murari *et al.* proposed a disruption prediction method using the SVM [8–10] and found three best SVMs [9]. Farias *et al.* attempted to predict the time to the occurrence of a disruption using multilayer NNs and multilayer SVMs [11]. Yokoyama *et al.* also attempted to predict the disruption [7], and showed that the effective combination of parameters improves the prediction  
80 performance of the disruption risk. Vega *et al.* proposed the use of Venn predictor, a multi-probability classification system [12].

Tang *et al.* proposed a method using a Recurrent Neural Network (RNN), which treats time-series data [13]. Farias *et al.* proposed a method using Long Short-Term Memory (LSTM) (a type of RNN), which learns the normal state  
85 and detects the abnormal state using LSTM [14].

Although disruption has been extensively investigated, studies on unusual emissions are still scarce. To address this gap in knowledge, this study treats unusual emissions and seeks to predict them.

### 3. Prediction method

#### 90 3.1. Feature values

The luminance value of the frame is used as a feature value [15]. The width and the height of the original video frame are 352 and 240 pixels, respectively. The unique number of the video and the playing time are included at the top and the bottom of a video. As these are not related to the plasma phenomenon  
95 itself, we removed them and set the frame to the size of  $256 \times 128$  pixels. The frame was converted to a grayscale image and divided into  $64 \times 64$  blocks. This means that one block comprises four pixels in width and two pixels in height. By making the mean value of the luminance values of the pixels in a block a pixel value, a frame of  $64 \times 64$  pixels was obtained. A vector of 4,096 dimensions  
100 was obtained from the  $64 \times 64$  pixel frame. This was used as a feature vector. This procedure is shown in Fig. 6.

In addition, the value of each dimension was normalized by being divided by 255. A non-luminous frame was considered inappropriate to be included in a dataset; thus, frames with a mean luminance value less than 40 were excluded.

#### 105 3.2. Support vector machine

We used an SVM as a basic two-class classifier to classify input data as unusual or usual emissions [15]. As the data could not be classified linearly, some kernel function is used for the classification.

#### 3.3. Calculation of the probability

110 The method proposed by Nakagawa *et al.* estimates whether a frame contains an unusual emission [15]. If a frame contains an unusual emission, the value of the frame is one. If a frame does not contain an unusual emission, the value is zero. The values may change frame by frame and are difficult to use in prediction.

115 This study used the mean value of  $N$  frames as the probability of unusual emission. When the values of all  $N$  frames are zero, the probability is zero.

When the values of several frames are one, the probability is greater than zero. When the values of all N frames are one, the probability is one. The mean value of these values can function as the probability of unusual emission.

## 120 4. Experiment

### 4.1. Dataset

Videos on LHD of NIFS were used. Visible light is frequently observed inside the plasma vessel during high-temperature plasma discharge experiments, which have been conducted at NIFS. The images of the visible light inside the vessel  
125 have been stored in disk devices at NIFS in the MPEG-1 format with a frame rate of 29.97 frames/sec. NIFS provided the plasma videos used herein.

The videos used were obtained from the plasma experiment in the 10th experimental campaign. Unusual visible light emission is sometimes observed in the plasma vessel under certain plasma discharge conditions. A bright flash  
130 can be observed on the internal sidewall when an unusual emission occurs. This bright flash is defined as a sequence of more than 10 frames, including the points whose colors are as shown in Eq. (1) in the Hue-Saturation-Value color space:

$$\begin{aligned} 55 &\leq Hue \leq 63 \\ 25 &\leq Saturation \leq 35 \\ Value &= 100 \end{aligned} \tag{1}$$

Examples with and without unusual emissions are shown in Fig. 7. Figs. 7(a) - (c) show examples with unusual emissions. Fig. 7(d) - (f) show examples  
135 without unusual emissions.

This study used 199 unusual emission videos and 254 videos without unusual emissions. A video containing unusual emission also contains some frames of non-unusual emission from before the start of the unusual emission. A total of 27,681 frames were obtained as the dataset. Of them, 7,968 frames included  
140 unusual emission (positive examples), while 19,713 frames did not (negative examples).

## 4.2. Experimental method

The dataset was prepared for learning an SVM. For machine learning, the dataset was divided into 2 : 8 for the test and training datasets.

145 The overview of the three-step experiment is shown in Fig. 8. The first step comprised training. The SVM was trained using the training dataset. After training, the SVM worked as a predictor of unusual emission. The second step comprised evaluation. The test dataset was used to evaluate the predictor through the metrics described in 4.3.1. The third step comprised examination,  
150 in which the effectiveness of the probability was examined. For the examination, six unusual emission videos and six videos without unusual emissions were selected at random from the videos correctly predicted in the second step. In this paper, we included a maximum of 12 videos to explain the examination result. The predictor used these videos, and the probability of occurrence of  
155 unusual emissions was calculated.

A Python machine learning library scikit-learn [20] was used for implementing the SVM. The Gaussian kernel was set for the SVM kernel function. In addition, the grid search method was applied to 1,431 examples randomly selected by varying the parameter  $\gamma$  of the Gaussian kernel in the range of 0.05,  
160 0.1, and 0.5. The cost parameter C varied in the range of 0.1, 1, and 10. This study set  $\gamma=0.05$  and  $C = 10$  with the highest evaluation values as SVM parameters.

## 4.3. Evaluation methods

### 4.3.1. Metrics for evaluation

165 Accuracy, precision, and recall were used as metrics for evaluating the learning results. These results were used in classification and information retrieval to show the soundness of classification and retrieval. Here two-class classification is treated, i.e., Yes (Positive) or No (Negative). Accuracy refers to the ratio of the number of instances correctly classified to the number of all instances. Precision  
170 refers to the degree to which positive instances are included in the instances

examined. Recall refers to the degree to which positive instances are obtained from all positive instances. These are defined by Eqs. (2) - (4), respectively.

$$Accuracy = \frac{TP + TN}{TP + FN + FP + TN} \quad (2)$$

$$Precision = \frac{TP}{TP + FP} \quad (3)$$

$$Recall = \frac{TP}{TP + FN} \quad (4)$$

where,  $TP$  is the number of examples correctly judged as positive examples;  $FN$  is the number of positive examples judged as negative examples by mistake;  $FP$  is the number of negative examples judged as positive examples by mistake; and  $TN$  is the number of negative examples correctly judged as negative examples. In the SVM, if the output of the prediction is one, the output is regarded as positive.

When there is no mistake, i.e.,  $FN$  and  $FP$  are equal to zero, accuracy is 1.0, i.e., 100 %. On the other hand, when there is no positive example judged as a negative example by mistake (or vice-versa), precision (recall) is 1.0 even if there are some negative examples judged as positive examples by mistake (or vice-versa).

#### 4.3.2. Prediction examination

To examine the performance of the predictor, the probability of unusual emission was calculated for 12 examination videos. Here, we used five as  $N$ , which is the number of frames used to calculate the probability. We calculated the probability using five frames by five frames.

### 4.4. Results

#### 4.4.1. Evaluation results

The confusion matrix of the test data is shown in Table 1. The numbers of false negatives and false positives are 93 and 107, respectively. Among 5537 frames, 200 frames were wrongly predicted .

The evaluation values of the test data are shown in Table 2. All values of  
195 metrics are over 0.9, which are remarkably high since 0.8 is usually considered  
high in the information retrieval and machine learning research areas. This  
means that unusual emissions were correctly predicted.

#### 4.4.2. Examination results

The probabilities of unusual emissions obtained are shown in Figs. 9 and 10  
200 for unusual and usual emissions, respectively. The number on the top of each  
graph indicates the serial number of the video. The horizontal axis shows the  
last frame number of the frames used in taking a mean value. As we used five  
frames in taking the mean value ( $N = 5$ ), the number on the axis is the frame  
number of the 5th frame. The graphs shown in Figs. 8 to 9 begin at five. This  
205 means that the 1st point of the graph is the mean value of the 1st to the 5th  
frame. The vertical axis represents the probability of unusual emission. The  
unusual emission began at one to four frames after the last frame of each graph  
shown in Fig. 9. For example, the unusual emission began at the 31st to the  
34th frame of the video, whose serial number is 2007-1-2373676 shown in Fig.  
210 9(a), where the last frame in the graph is the 30th frame.

According to Figs. 9(a) - 9(f), unusual emission is predicted in the SVM  
the moment before its start. In addition, the probability of unusual emission  
becomes high in 10 or more frames. Except for Fig. 9(c), this is maintained  
until just before the start point of the unusual emission.

215 According to Figs. 10(a) - 10(f), the probability of unusual emission is low  
for videos that do not include unusual emissions.

## 5. Discussion

### 5.1. Prediction performance

As shown in Table 2, the recall is higher than the precision. This means that  
220 there are few false dismissals, which are unusual but reported as not unusual.

Although the difference between precision and recall is not expressive, this tendency is preferable because it is required that unusual emissions be correctly predicted.

Although 200 frames were wrongly predicted, their ratio to all 5537 frames  
225 is considerably small. This can be understood by 0.964 of accuracy.

### 5.2. Prediction of unusual emissions

Let us consider 0.8 or more of the probability as high probability. Two or more consecutive mean values whose values are 0.8 are seen in Figs. 9(a) - 9(f). Although the probability mean values just before the unusual emission  
230 of Figs. 9(c) and 9(e) were less than 1.0, unusual emission can successfully be predicted because two consecutive high mean values appeared before the unusual emission. As five frames were used in calculating the mean value ( $N = 5$ ) in this experiment, two consecutive mean points mean ten consecutive frames. Therefore, ten consecutive frames whose mean values of every five frames are  
235 equal to or more than 0.8 may be the criterion to trigger an alarm of unusual emission. This means that it takes approximately 0.3 seconds to trigger an alarm because the frame rate is around 30 frames/second. This also means that an unusual emission can be predicted approximately 0.3 seconds before it begins.

240 Although the graphs shown in Fig. 9 report the correct prediction, this does not mean that there is no prediction failure. An example of prediction failure is shown in Fig. 11. After the 30th frames, the probability remained zero.

Figs. 10(a), 10(c), and 10(d) show that the probabilities of unusual emission are higher than zero at some frames. These are, however, only seen at the  
245 beginning of plasma emissions.

From these results, the SVM is considered effective in predicting unusual emissions. It can trigger an alarm of an unusual emission approximately 0.3 seconds before it begins. It is considered that the luminance value of the frame is effective as a feature value in predicting unusual emissions.

250 *5.3. Machine learning methods*

As previously mentioned, NNs are often used in machine learning. Although it is often said that an NN attains good estimation performance and that feature values are not required, an NN needs considerable training data (usually 100,000 or more data). We used approximately 22,000 data, which may not be sufficient  
255 for an NN. As the literature reports that several hundreds of data are sufficient for the SVM [21], our data are sufficient for the SVM.

Nakagawa *et al.* used a Hidden Markov Model (HMM) to estimate a plasma transition, which is the transition of visible light inside the plasma vessel [16]. As an HMM treats time series data, the prediction in this paper may be treated  
260 by using an HMM. However, an HMM is more difficult to be used than an SVM. An HMM does not always attain better performance than an SVM [22]. If an SVM attains good prediction performance, an SVM is preferred.

## 6. Conclusion

We proposed a method for predicting unusual emission of a plasma video.  
265 A predictor was constructed by learning with the SVM, using the frames of plasma videos with or without unusual emissions. Accuracy, precision, and recall were used as evaluation metrics. High accuracy and high precision were obtained with the proposed machine learning method. This study confirmed experimentally whether an unusual emission could be predicted in advance by  
270 using the predictor. It was shown that the SVM is effective in predicting unusual emissions before they start. It was also found that the luminance value of the frame is effective as a feature value for predicting unusual emissions.

Although the precision of the prediction is remarkably high, the prediction of unusual emissions still fails. When we attempt to achieve complete prediction,  
275 that is, no prediction failure, precision usually degrades. Therefore, achieving higher recall with keeping high precision is the scope for further research. We used the luminance value as the feature value. Although the luminance value works well for the prediction of the unusual emission, there may be other values

suitable to feature values. Identifying the characteristics of plasma videos for more  
280 effective prediction should be included in future studies, as this may improve  
the recall of the prediction.

### Acknowledgment

This research is partly supported by the National Institute for Fusion Science  
under NIFS15KLEH046 and NIFS19KLEH079.

### 285 References

- [1] Large Helical Device Project Home Page, <http://www.lhd.nifs.ac.jp/>, (reference 3-26-2019).
- [2] M. Shoji, K. Yamazaki, and S. Yamaguchi, "Development of the Real-time Image Data Acquisition System for Observing the Plasma Dynamic Behavior of LHD Long-pulse Discharges," *Journal of Plasma and Fusion Research SERIES*, vol. 3, pp. 440–443, 2000.
- [3] J. Vega, A. Murari, S. Dormido-Canto, R. Moreno, A. Pereira, S. Esquem-bri, and JET Contributors, "Real-time anomaly detection for disruption prediction: the JET case," *EUROfusion*, WPJET1-PR(16), 14855, 2014.
- 295 [4] R. Moreno, J. Vega, A. Murari, and JET EFDA contributors, "Automatic Location of Disruption Times in JET," *EFDA-JET*, EFDA-JET-PR(14)14, 2014.
- [5] J. González, M. Ruiz, J. Vega, E. Barrera, G. Arcas, and J. M. López, "Event recognition using signal spectrograms in long pulse experiments," *Review of Scientific Instruments*, vol. 81, 10E126, 2010.
- 300 [6] J. Vega, R. Moreno, A. Pereira, S. Dormido-Canto, A. Murari, and JET Contributors, "Advanced Disruption Predictor Based on the Locked Mode signal: Application to JET, Proceedings of Science, Proceedings of 1st EPs Conference on Plasma Diagnostics (1st ECPD)," 2015.

- 305 [7] T. Yokoyama, T. Sueyoshi, Y. Miyoshi, R. Hiwatari, Y. Igarashi, M. Okada,  
and Y. Ogawa, “Disruption Prediction by Support Vector Machine and  
Neural Network with Exhaustive Search,” *Plasma and Fusion Research*,  
vol. 13, 3405021, pp. 1–4, 2018.
- [8] A. Murari, J. Vega, D. Mazon, G.A. Rattá, J. Svensson, G. Vagliasindi,  
310 J. Blum, C. Boulbe, B. Faugerat, and JET-EFDA Contributors, “New  
information processing methods for control on JET,” *Fusion Engineering  
and Design*, vol. 85. pp. 428–432, 2010.
- [9] A. Murari, J. Vega, D. Mazon, G.A. Rattá, J. Svensson, S. Palazzo, G.  
Vagliasindi, P. Arena, C. Boulbe, B. Faugeras, L. Fortuna, D. Moreau and  
315 JET-EFDA Contributors, “Innovative signal processing and data analysis  
methods on JET for control in the perspective of next-step devices,” *Nucl.  
Fusion*, vol. 50, 055005, 2010.
- [10] J. Vega, S. Dormido-Canto, J. M. López, A. Murari, J. M. Ramírez, R.  
Moreno, M. Ruiz, D. Alves, R. Felton, and JET-EFDA Contributors, “Re-  
320 sults of the JET real-time disruption predictor in the ITER-like wall cam-  
paigns,” *Fusion Engineering and Design*, vol. 88, pp. 1228–1231, 2013.
- [11] G. Farias, J. Vega, S. Dormido-Canto, A. Murari, R. Moreno, H. Vargas, A.  
Valencia, and JET EFDA contributors, “Prediction of the Time to Disrup-  
tion in JET with an ITER-Like Wall,” *EFDA-JET, EFDA-JET-PR(14)08*,  
325 2014.
- [12] J. Vega, A. Murari, S. Dormido-Canto, R. Moreno, A. Pereira, A. Acero,  
and JET EFDA contributors, “Adaptive High Learning Rate Probabilistic  
Disruption Predictors from Scratch for the Next Generation of Tokamaks,”  
*EFDA-JET-PR(13)44*, 2013.
- 330 [13] W. Tang, M. Parsons, E. Feibush, J. Choi, T. Kurc, A. Murari, J. Vega,  
A. Pereira, I. Nunes, and JET contributors, “Big Data Machine Learning  
for Disruption Predictions,” *EUROfusion, WPJET1-CP(16),15330*, 2016.

- [14] G. Farias, E. Fabregas, S. Dormido-Canto, J. Vega, S. Vergara, “Automatic recognition of anomalous patterns in discharges by recurrent neural networks,” Fusion Engineering and Design, vol. 154, 111495, 2020.
- [15] S. Nakagawa, T. Hochin, H. Nomiya, H. Nakanishi, and M. Shoji, “Prediction of Abnormal Plasma Discharge through Machine Learning,” Proc. of 6th International Conference on Computational Science/Intelligence & Applied Informatics (CSII 2019), pp. 7–12, 2019.
- [16] S. Nakagawa, T. Hochin, H. Nomiya, and H. Nakanishi, “Estimation of Plasma Emission Transition Using Hidden Markov Model,” Plasma and Fusion Research, vol. 13, 3405117, pp. 1–6, 2018.
- [17] S. Nakagawa, T. Hochin, H. Nomiya, and H. Nakanishi, “Estimation of Plasma Emission Transition Using Clustered Time Series Data,” Proc. of 31st International Conference on Computer Applications in Industry and Engineering (CAINE 2018), pp. 201-206, 2018.
- [18] N. Noda, “LHD Divertor,” <http://www.interq.or.jp/www1/nodanob/Japanese/LHD-Divertor/>, (reference December 30, 2020). (in Japanese).
- [19] V. N. Vapnik, “The Nature of Statistic Learning Theory,” Springer Science & Business Media New York, 1995.
- [20] scikit-learn: <https://scikit-learn.org/stable/index.html>, (reference March 26, 2019).
- [21] D. Meyer, F. Leash, K. Hornik, “The support vector machine under test,” Neurocomputing, vol. 55, pp. 169-186, 2003.
- [22] E. J. R. Justino, F. Bortolozzi, R. Sabourin, “A comparison of SVM and HMM classifiers in the off-line signature verification,” Pattern Recognition Letters, vol. 26, no. 9, pp. 1377-1385, 2005.

Table 1: Confusion matrix of test data

Actual	prediction (positive)	prediction (negative)
data (positive)	1,462	93
data (negative)	107	3,875

Table 2: Evaluation values of test data

model	accuracy	precision	recall
SVM	0.964	0.932	0.940

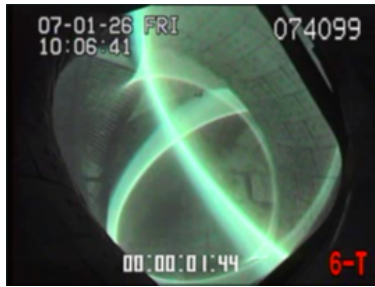


Figure 1: Example of a scene of a plasma video



Figure 2: Example of the light reflected from the divertor tiles

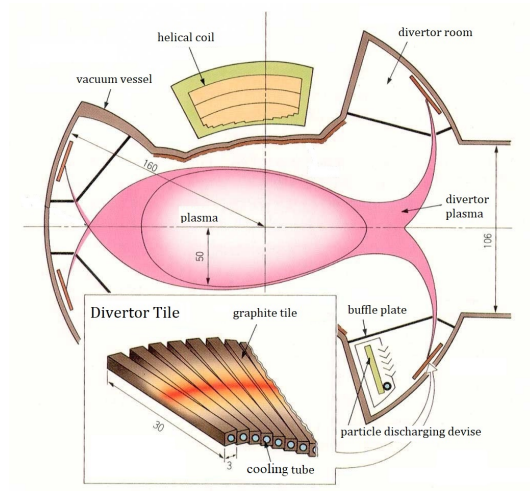


Figure 3: Sectional view of the Large Helical Device (LHD) including divertors [18].

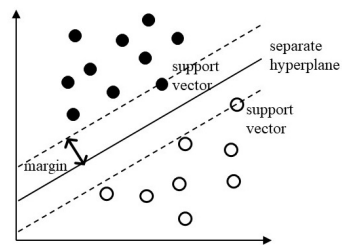


Figure 4: Support vector machine (SVM)

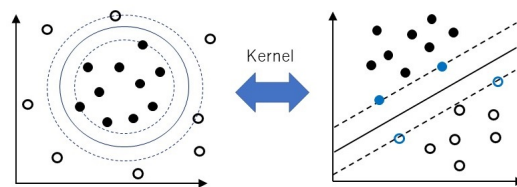


Figure 5: Kernel of support vector machine

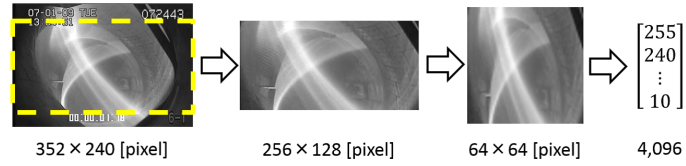


Figure 6: Procedure of feature extraction

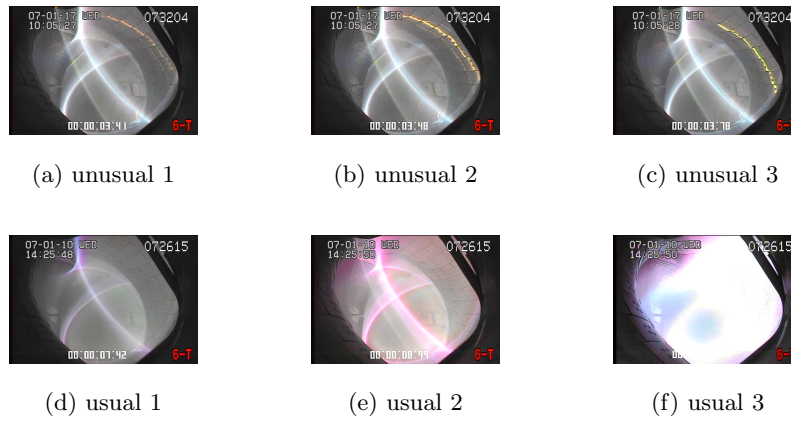


Figure 7: Examples of frames in the dataset

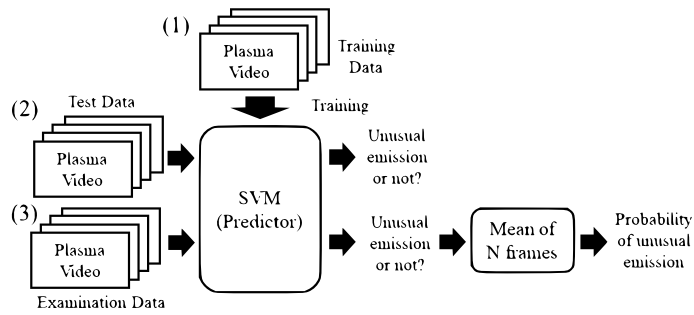
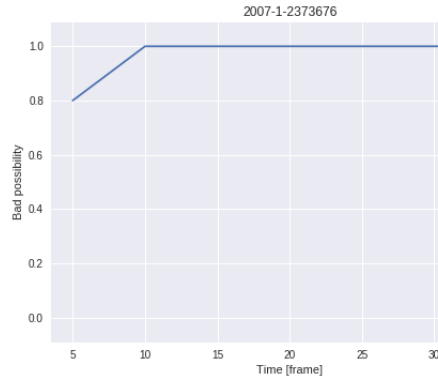
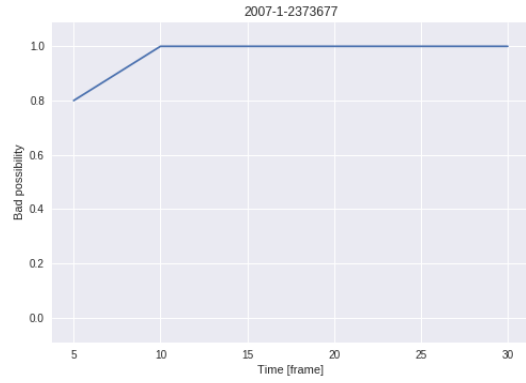


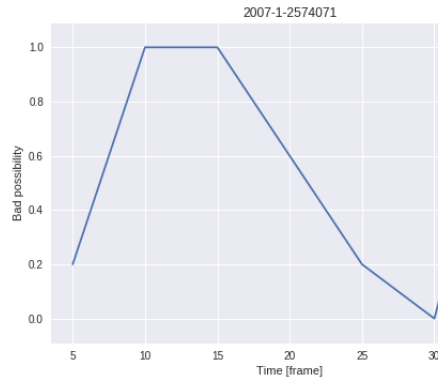
Figure 8: Overview of experiment



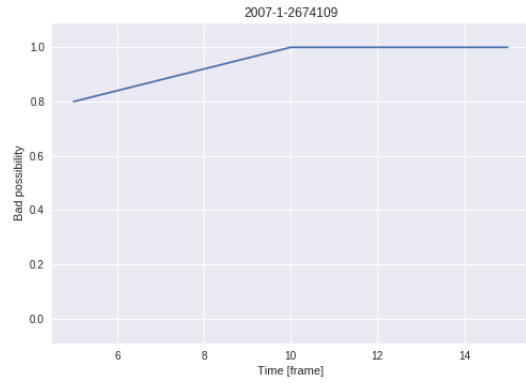
(a) 2007-1-2373676



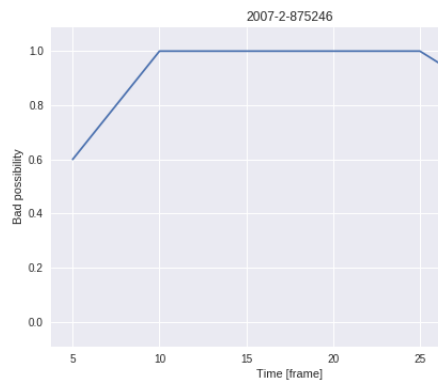
(b) 2007-1-2373677



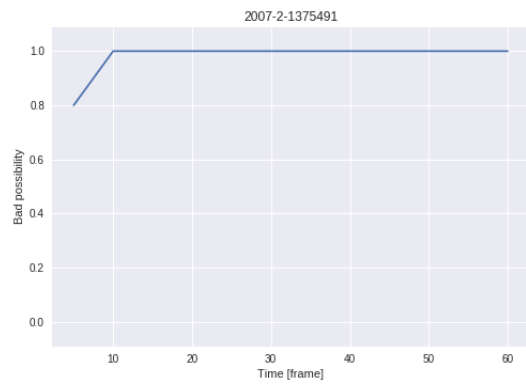
(c) 2007-1-2574071



(d) 2007-1-2674109

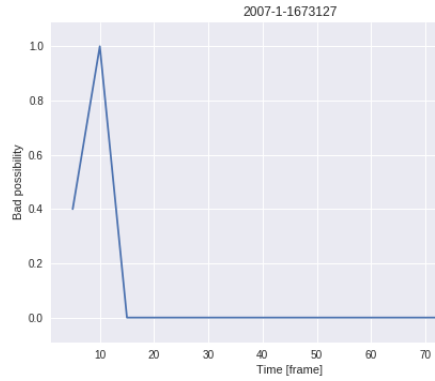


(e) 2007-2-875246

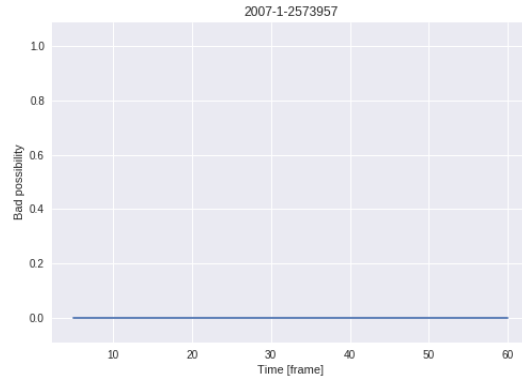


(f) 2007-2-1375491

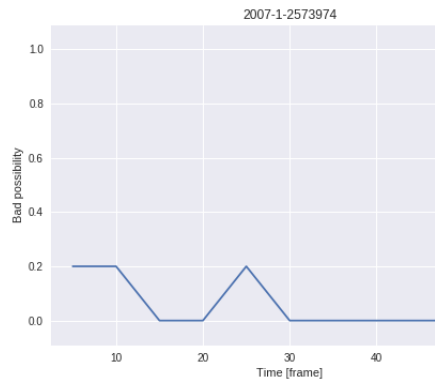
Figure 9: Prediction results (unusual emission)



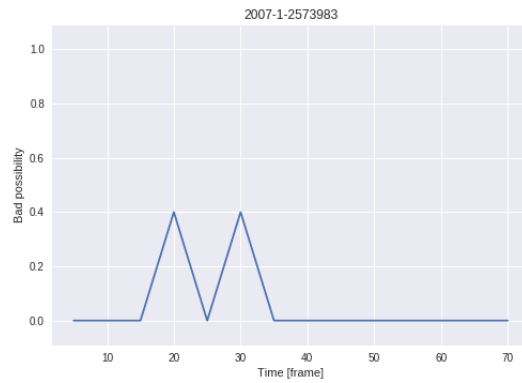
(a) 2007-1-1673127



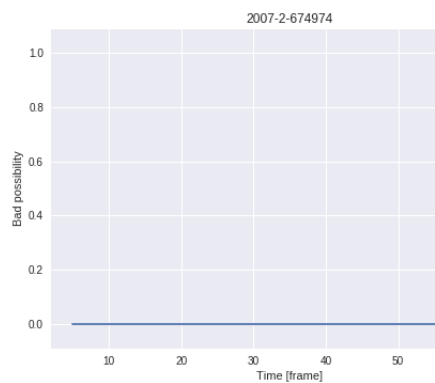
(b) 2007-1-2573957



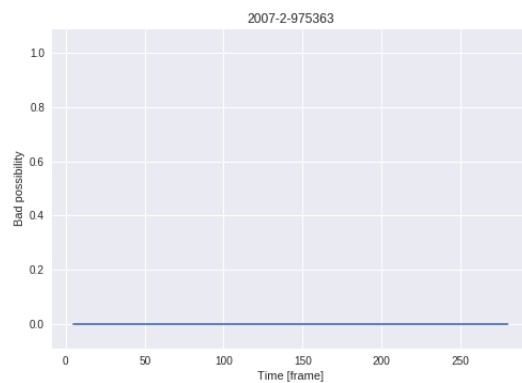
(c) 2007-1-2573974



(d) 2007-1-2573983



(e) 2007-2-674974



(f) 2007-2-975363

Figure 10: Prediction results (usual emission)

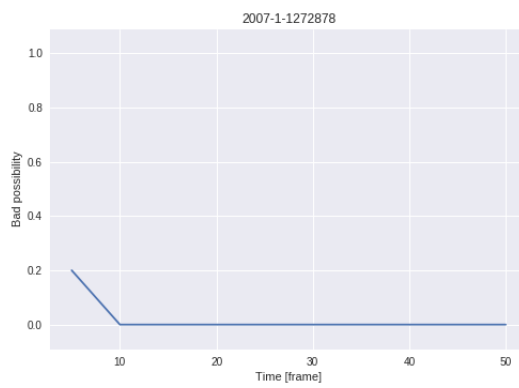


Figure 11: A failed prediction example (unusual emission)